Advances in Applied Mathematics and Mechanics
Adv. Appl. Math. Mech., Vol. **6**, No. 3, pp. 359-375

DOI: 10.4208/aamm.2013.m303
June 2014

Mixed Convection in Viscoelastic Boundary Layer Flow and Heat Transfer Over a Stretching Sheet

Antonio Mastroberardino*

School of Science, Penn State Erie, The Behrend College, Erie, Pennsylvania 16563, USA

Received 25 July 2013; Accepted (in revised version) 9 January 2014

Available online 21 May 2014

Abstract. An investigation is carried out on mixed convection boundary layer flow of an incompressible and electrically conducting viscoelastic fluid over a linearly stretching surface in which the heat transfer includes the effects of viscous dissipation, elastic deformation, thermal radiation, and non-uniform heat source/sink for two general types of non-isothermal boundary conditions. The governing partial differential equations for the fluid flow and temperature are reduced to a nonlinear system of ordinary differential equations which are solved analytically using the homotopy analysis method (HAM). Graphical and numerical demonstrations of the convergence of the HAM solutions are provided, and the effects of various parameters on the skin friction coefficient and wall heat transfer are tabulated. In addition it is demonstrated that previously reported solutions of the thermal energy equation given in [1] do not converge at the boundary, and therefore, the boundary derivatives reported are not correct.

AMS subject classifications: 76D10, 76W05

Key words: Viscoelastic fluid, non-uniform heat source/sink, viscous dissipation, thermal radiation, homotopy analysis method.

1 Introduction

More than 100 years after Blasius equation was formulated to describe the boundary layer present in uniform viscous flow over a semi-infinite plate [2], researchers in engineering and applied mathematics continue to investigate the nonlinear differential equations that describe boundary layer flow. Since the landmark work of Blasius, variations of the classical problem have been formulated that consider different flow scenarios and incorporate relevant physical phenomena. In practically all cases considered, the differential equations governing the flow are nonlinear, and the existence of exact solutions is

*Corresponding author.
Email: axm62@psu.edu (A. Mastroberardino)

rare. As such numerous analytical methods–one of the earliest being the classical perturbation methods–have been developed over the years in order to find approximate solutions. Singular perturbation theory, which is appropriate in the analysis of boundary layer flow, has had a profound impact in the applied sciences and, in particular, quantum physics as evidenced by its vast use over the past 100 years.

As successful as the perturbation methods have been, they have the drawback of relying on the existence of a small or large parameter to be valid. Because of this drawback, various alternative analytical techniques have been developed over the past several decades that do not rely on the existence of a small or large parameter. This paper highlights one of these techniques, namely the homotopy analysis method (HAM) [3–10], which has proven to be a valuable tool in solving not only the nonlinear differential equations of fluid mechanics but also in solving numerous other problems arising in engineering, finance, and the applied sciences. In comparison to other analytical methods, HAM offers the ability to adjust and control the convergence of a solution via the so-called convergence-control parameter.

In a study of two-dimensional boundary layer flow over a moving surface in a fluid at rest, Sakiadis [11] demonstrated that the flow was governed by Blasius equation with different boundary conditions than the Blasius flow. The results of this study were later extended by Crane [12] to include an exact analytical solution for the case of a linearly stretching sheet. It is worth noting that both of these studies consider a Newtonian fluid in the analysis. In recent years, research on the fluid dynamics and heat transfer of boundary layer flow involving non-Newtonian fluids has received increased attention due their growing importance in numerous industrial and biomedical applications. The mechanical properties of the products involved in these applications can be substantially altered by the rate of stretching, rate of cooling, application of a magnetic field, etc., and so, understanding the viscous and thermal characteristics of non-Newtonian fluids is paramount.

Of particular interest is a subclass of non-Newtonian fluids called viscoelastic fluids. Vajravelu and Rollins [13] investigated the fluid flow and heat transfer of a second-order fluid over a stretching sheet with viscous dissipation and internal heat source/sink. Sarma and Rao [14] extended these results by including the effects of work due to elastic deformation, noting that the exclusion of this effect is not in accordance with the inclusion of viscous dissipation. Pillai et al. [15] provided a similar analysis for the flow of a Walters' liquid B fluid in a porous medium. Abel et al. [16] considered the effects of viscous dissipation and a non-uniform heat source/sink on the flow and heat transfer characteristics of a Walters' liquid B fluid. Arnold et al. [17] and Nandeppanavar et al. [1] followed with similar studies by incorporating work due to deformation.

In various engineering processes, it is well understood that thermal radiation plays a significant role when operating temperatures are high. For example in the design of advanced energy conversion systems [18], effects of thermal radiation on the flow and heat transfer characteristics can be quite significant. Raptis and Perdikis [19] were the first to study the effects of thermal radiation on viscoelastic boundary layer flow. A recent study

by Chen [20] considered thermal radiation along with viscous dissipation, internal heat source/sink, and work done by elastic deformation performed a permeable sheet subject to a uniform magnetic field. Nandeppanavar et al. [21] preformed a similar analysis in which they considered non-uniform internal heat source/sink.

All of the aforementioned studies considered forced convection as the sole mode of heat transfer. In this work, the effects of free convection for viscoelastic boundary layer flow and heat transfer over a stretching permeable sheet in which the heat transfer analysis includes viscous dissipation, elastic deformation, thermal radiation, and non-uniform heat source/sink are investigated. Free convection becomes important when the temperature difference between the sheet and the ambient fluid is large enough to cause density gradients in the fluid creating a buoyancy force [22] that is of the same magnitude as the inertial force. The governing nonlinear partial differential equations for the velocity field and temperature field are transformed to a coupled system of nonlinear ordinary differential equations which is solved using the homotopy analysis method (HAM). The results of this study are then compared to those obtained by Nandeppanavar et al. [1] in which only forced convection is considered. It is clearly demonstrated that the analytical solutions of the temperature field given in terms of Kummer's function in [1] do not converge at the boundary, and thus, do not provide accurate values of the wall temperature and wall temperature gradient for the boundary conditions in consideration.

These results clearly demonstrate that HAM is worthy of consideration by researchers who seek analytical solutions to problems involving viscoelastic boundary layer flow and heat transfer. It is worth mentioning that HAM has recently been applied to solve various problems that consider mixed convection as part of the analysis [23–29]. Under this scenario, there is a two-way coupling between the governing momentum equation and thermal equation and the conventional analytical method of solution that involves an exact solution for the velocity field and a solution in terms of Kummer's function for the temperature field no longer applies.

2 Fluid flow analysis

Consider a two-dimensional flow field that is induced by the motion of a linearly stretching sheet in which an incompressible and electrically conducting viscoelastic fluid is subject to a transverse uniform magnetic field. Two equal and opposite forces are applied along the sheet so that it is stretched with a velocity that is proportional to the distance from the origin. The plane $y=0$ is taken to be parallel to the motion of the sheet, and, because of symmetry, the fluid is considered to occupy the half space $y>0$.

The continuity equation and momentum equations for viscoelastic boundary layer flow, first derived by Beard and Walters [30], are given by

$$\frac{\partial u}{\partial x}+\frac{\partial v}{\partial y}=0, \tag{2.1a}$$

$$u\frac{\partial u}{\partial x}+v\frac{\partial u}{\partial y}=\nu\frac{\partial^2 u}{\partial y^2}-k_0\Big\{u\frac{\partial^3 u}{\partial x\partial y^2}+v\frac{\partial^3 u}{\partial y^3}+\frac{\partial u}{\partial x}\frac{\partial^2 u}{\partial y^2}-\frac{\partial u}{\partial y}\frac{\partial^2 u}{\partial x\partial y}\Big\}+g\beta(T-T_\infty), \tag{2.1b}$$

where u and v are the velocities in the x and y directions, respectively, ν is the kinematic viscosity, k_0 is the viscoelastic parameter, g is the acceleration due to gravity, β is the thermal expansion coefficient, T is the temperature of the fluid, and T_∞ is the ambient temperature. To derive these equations, it is assumed that the contribution of the normal stress is of the same order as the shear stress. The appropriate boundary conditions for the velocity field are given by

$$u_w=bx,\quad v=0 \qquad \text{at } y=0, \tag{2.2a}$$

$$u\to 0,\qquad u_y\to 0 \quad \text{as } y\to\infty, \tag{2.2b}$$

where b is the rate of stretching.

The governing thermal boundary layer equation in the presence of viscous dissipation, elastic deformation, non-uniform internal heat source/sink, and thermal radiation for two-dimensional flow is

$$u\frac{\partial T}{\partial x}+v\frac{\partial T}{\partial y}=\alpha^*\frac{\partial^2 T}{\partial y^2}+\frac{\nu}{C_p}\Big(\frac{\partial u}{\partial y}\Big)^2-\frac{1}{\rho C_p}\frac{\partial q_r}{\partial y}+\frac{k_0}{C_p}\Big\{\frac{\partial u}{\partial y}\frac{\partial}{\partial y}\Big(u\frac{\partial u}{\partial x}+v\frac{\partial u}{\partial y}\Big)\Big\}+\frac{q'''}{\rho C_p}, \tag{2.3}$$

where C_p is the specific heat at constant pressure, and α^* is the thermal diffusivity. The non-uniform internal heat source/sink with spatial and temperature dependence is given by [1]

$$q'''=\frac{kb}{\nu}\Big[A^*(T_w-T_\infty)\frac{u}{u_w}+B^*(T-T_\infty)\Big], \tag{2.4}$$

where k is the thermal conductivity, T_w is the wall temperature, and A^* and B^* are parameters related to the spatial and temporal dependent heat source/sink, respectively.

Assuming the Rosseland approximation [32], the radiative heat flux is given by

$$q_r=-\frac{4\sigma^*}{3k^*}\frac{\partial(T^4)}{\partial y}, \tag{2.5}$$

where σ^* is the Stefan-Boltzmann constant and k^* is the mean absorption coefficient. The temperature differences within the flow are assumed to be small enough so that T^4 can be approximated by a linear function, which is obtained by expanding T^4 in a Taylor series about T_∞ and neglecting higher order terms, yielding

$$T^4\approx -3T_\infty^4+4T_\infty^3T. \tag{2.6}$$

Substituting (2.4)-(2.6) into Eq. (2.3) yields

$$u\frac{\partial T}{\partial x}+v\frac{\partial T}{\partial y}=\Big(\alpha^*+\frac{16\sigma^*T_\infty^3}{3\rho C_pk^*}\Big)\frac{\partial^2 T}{\partial y^2}+\frac{\nu}{C_p}\Big(\frac{\partial u}{\partial y}\Big)^2+\frac{k_0}{C_p}\Big\{\frac{\partial u}{\partial y}\frac{\partial}{\partial y}\Big(u\frac{\partial u}{\partial x}+v\frac{\partial u}{\partial y}\Big)\Big\}+\frac{q'''}{\rho C_p}. \tag{2.7}$$

2.1 Prescribed surface temperature

The boundary conditions for the temperature field in the case of a prescribed surface temperature (PST) that is quadratic in x are given by

$$T = T_w = T_\infty + A\left(\frac{x}{l}\right)^2 \qquad \text{at } y = 0, \tag{2.8a}$$

$$T \to T_\infty \qquad \text{as } y \to \infty, \tag{2.8b}$$

where A is a constant that depends on the thermal properties of the fluid and l is a characteristic length.

Eqs. (2.1a), (2.1b) and (2.7) can be transformed into a system of ordinary differential equations by defining

$$u = bxf'(\eta), \qquad v = -\sqrt{b\nu}f(\eta), \qquad \eta = \sqrt{\frac{b}{\nu}}y, \tag{2.9a}$$

$$\theta(\eta) = \frac{T - T_\infty}{T_w - T_\infty}. \tag{2.9b}$$

Substituting (2.9a)-(2.9b) into Eqs. (2.1a), (2.1b), and (2.7) yields the nonlinear system

$$f''' - f'^2 + ff'' - k_1(2f'f''' - f''^2 - ff'''') - \lambda\theta = 0, \tag{2.10a}$$

$$(1+Nr)\theta'' + Prf\theta' + (B^* - 2Prf')\theta + EcPr(f''^2 - k_1 f''(f'f'' - ff''')) + A^* f' = 0, \tag{2.10b}$$

where the non-dimensional parameters are defined as follows:

$$k_1 = \frac{bk_0}{\nu} \qquad \text{viscoelastic parameter,}$$

$$\lambda = \frac{g\beta(T_w - T_\infty)x^3/\nu^2}{u_w^2 x^2/\nu^2} \qquad \text{free convection parameter,}$$

$$Nr = \frac{16\sigma^* T_\infty^3}{3\rho C_p k^*} \qquad \text{thermal radiation parameter,}$$

$$Pr = \frac{\nu}{\alpha^*} \qquad \text{Prandtl number,}$$

$$Ec = \frac{b^2 l^2}{AC_p} \qquad \text{Eckert number.}$$

Due to its dependence on x, the free convection parameter is considered to be a local parameter and the transformation of the governing differential equations a local similarity. The boundary conditions in (2.2b) and (2.8b) become

$$f(0) = 0, \qquad f'(0) = 1, \qquad f'(\infty) = 0, \qquad f''(\infty) = 0, \tag{2.11a}$$

$$\theta(0) = 1, \qquad \theta(\infty) = 0. \tag{2.11b}$$

Regarding the physical quantities of interest, the wall shearing stress τ_w on the surface of the stretching sheet is given by

$$\tau_w = \Big[\nu\frac{\partial u}{\partial y} - k_0\Big(u\frac{\partial^2 u}{\partial x\partial y} - 2\frac{\partial u}{\partial x}\frac{\partial u}{\partial y}\Big)\Big]_{y=0}. \tag{2.12}$$

Substituting (2.12) into the the expression for the local skin friction coefficient yields

$$C_f = \frac{\tau_w}{\frac{1}{2}\rho u_w^2} = \frac{2}{\sqrt{Re_x}}(1-3k_1)f''(0), \tag{2.13}$$

where $Re_x = u_w x/\nu$ is the local Reynolds number. The local heat flux is given by

$$q_w = -k\Big(\frac{\partial T}{\partial y}\Big)_{y=0} = -k\sqrt{\frac{b}{\nu}}(T_w - T_\infty)\theta'(0), \tag{2.14}$$

where $\theta'(0)$ is the nondimensional wall temperature gradient.

2.2 Prescribed heat flux

The boundary conditions for the temperature field for the case of a prescribed power law surface heat flux (PHF) that is quadratic in x are given by

$$-k\frac{\partial T}{\partial y} = q_w = D\Big(\frac{x}{l}\Big)^2 \qquad \text{at } y=0, \tag{2.15a}$$

$$T \to T_\infty \qquad \text{as } y\to\infty, \tag{2.15b}$$

where D is a constant that depends on the thermal properties of the fluid.

Substituting

$$g(\eta) = \frac{T-T_\infty}{T_w - T_\infty}, \tag{2.16}$$

where

$$T_w - T_\infty = \frac{D}{k}\Big(\frac{x}{l}\Big)^2\sqrt{\frac{\nu}{c}}$$

into Eq. (2.7) yields

$$(1+Nr)g'' + Prfg' + (B^* - 2Prf')g + EcPr(f''^2 - k_1 f''(f'f'' - ff''')) + A^* f' = 0, \tag{2.17}$$

where $Ec = kb^2l^2\sqrt{b/\nu}/DC_p$ is the Eckert number in the PHF case.

The boundary conditions in (2.15b) become

$$g'(0) = -1, \qquad g(\infty) = 0. \tag{2.18}$$

The wall temperature is given by

$$T_w = T_\infty + \frac{q_w}{k}\sqrt{\frac{\nu}{b}}g(0). \tag{2.19}$$

3 Homotopy analysis method

The homotopy analysis method (HAM) was formulated by Liao in his doctoral thesis [3] and then modified [4] to incorporate into the solution expression the use of the so-called convergence-control parameter, a distinguishing feature of the method. To apply a basic version of HAM, one constructs the zeroth-order deformation equation which includes the choice of an auxiliary linear operator, a nonlinear operator, and an initial guess that satisfies the initial and/or boundary conditions. The auxiliary linear operator is chosen so as to obtain a solution expression in terms of elementary functions that will best capture the expected behavior of the solution. The nonlinear operator is usually, but not always, equivalent to the nonlinear equation that one is attempting to solve. See [9,10] for examples in which the nonlinear operator differs from the nonlinear differential equation in consideration.

Included in the zeroth-order deformation equation is the convergence-control parameter, which allows one to adjust the convergence of an approximate solution, and thus, offers greater ability to achieve convergence in comparison with other analytical methods. The value of the convergence-control parameter is determined after the solution expression is obtained by solving a sequence of linear differential equations, which are constructed by a procedure outlined below.

HAM is now applied to the nonlinear boundary value problem in (2.10a), (2.11a), (2.10b), and (2.11b) for $f(\eta)$ and $\theta(\eta)$ for the PST case. The procedure is essentially the same for PHF in which case (2.10b), (2.11b) and $\theta(\eta)$ are replaced by (2.17), (2.18) and $g(\eta)$, respectively. Any other differences will be explicitly noted. The linear operators are chosen to be

$$\mathcal{L}_f(f)=\frac{d^3f}{d\eta^3}-\frac{df}{d\eta},\qquad \mathcal{L}_\theta(\theta)=\frac{d^2\theta}{d\eta^2}-\theta, \tag{3.1}$$

and the nonlinear operators, $\mathcal{N}_f$ and $\mathcal{N}_\theta$, are chosen to match Eqs. (2.10a) and (2.10b), respectively. To satisfy the boundary conditions in (2.11a) and (2.11b), the initial guesses are chosen to be

$$f_0(\eta)=1-e^{-\eta}, \tag{3.2a}$$
$$\theta_0(\eta)=e^{-\eta}. \tag{3.2b}$$

The zeroth-order deformation equations are then

$$(1-q)\mathcal{L}_f\big[F(\eta,q)-f_0(\eta)\big]=q\hbar_f\mathcal{N}_f\big[F(\eta,q)\big], \tag{3.3a}$$
$$(1-q)\mathcal{L}_\theta\big[\Theta(\eta,q)-\theta_0(\eta)\big]=q\hbar_\theta\mathcal{N}_\theta\big[F(\eta,q),\Theta(\eta,q)\big], \tag{3.3b}$$

where the boundary conditions are given in (2.11a) and (2.11b). $\hbar_f$ and $\hbar_\theta$ are the convergence-control parameters and $q\in[0,1]$ is an embedding parameter such that

$$F(\eta,0)=f_0(\eta),\qquad F(\eta,1)=f(\eta), \tag{3.4a}$$
$$\Theta(\eta,0)=\theta_0(\eta),\qquad \Theta(\eta,1)=\theta(\eta). \tag{3.4b}$$

Note that as q increases from 0 to 1, $F(\eta,q)$ and $\Theta(\eta,q)$ vary from the initial guesses given in (3.2a)-(3.2b) to the desired solutions $f(\eta)$ and $\theta(\eta)$. A Taylor series expansion of $F(\eta,q)$ and $\Theta(\eta,q)$ with respect to q yields

$$F(\eta,q)=f_0(\eta)+\sum_{m=1}^{\infty}f_m(\eta)q^m, \tag{3.5a}$$

$$\Theta(\eta,q)=\theta_0(\eta)+\sum_{m=1}^{\infty}\theta_m(\eta)q^m, \tag{3.5b}$$

where

$$f_m(\eta)=\frac{1}{m!}\frac{\partial^m F(\eta,q)}{\partial q^m}\Big|_{q=0}, \qquad \theta_m(\eta)=\frac{1}{m!}\frac{\partial^m \Theta(\eta,q)}{\partial q^m}\Big|_{q=0}. \tag{3.6}$$

If the auxiliary linear operators, the initial guesses, and the convergence-control parameters are properly chosen so that the series in (3.5a)-(3.5b) all converge at $q=1$, the homotopy-series solutions given by

$$f(\eta)=f_0(\eta)+\sum_{m=1}^{\infty}f_m(\eta), \tag{3.7a}$$

$$\theta(\eta)=\theta_0(\eta)+\sum_{m=1}^{\infty}\theta_m(\eta), \tag{3.7b}$$

are obtained.

Differentiating Eqs. (3.3a)-(3.3b) m times with respect to the embedding parameter q, dividing by $m!$, and then setting $q=0$ yields the mth-order deformation equations given by

$$\mathcal{L}_f\left[f_m(\eta)-\chi_m f_{m-1}(\eta)\right]=\hbar_f R_m^f(\eta), \tag{3.8a}$$

$$\mathcal{L}_\theta\left[\theta_m(\eta)-\chi_m \theta_{m-1}(\eta)\right]=\hbar_\theta R_m^\theta(\eta), \tag{3.8b}$$

subject to the boundary conditions

$$f_m(0)=0, \qquad f_m'(0)=0, \qquad f_m'(\infty)=0, \qquad f_m''(\infty)=0, \tag{3.9a}$$

$$\theta_m(0)=0, \qquad \theta_m(\infty)=0 \qquad \text{for PST}, \tag{3.9b}$$

$$g_m'(0)=0, \qquad g_m(\infty)=0 \qquad \text{for PHF}, \tag{3.9c}$$

where

$$\begin{aligned}R_m^f(\eta)=f_{m-1}'''&-\sum_{n=0}^{m-1}f_n'f_{m-1-n}'+\sum_{n=0}^{m-1}f_nf_{m-1-n}''\\&-k_1\Big[2\sum_{n=0}^{m-1}f_n'f_{m-1-n}'''-\sum_{n=0}^{m-1}f_n''f_{m-1-n}''-\sum_{n=0}^{m-1}f_nf_{m-1-n}''''\Big],\end{aligned} \tag{3.10a}$$

$$R^{\theta}_m(\eta)=(1+Nr)\theta''_{m-1}+Pr\Big[\sum_{n=0}^{m-1}f_n\theta'_{m-1-n}-2\sum_{n=0}^{m-1}f'_n\theta_{m-1-n}\Big]+B^*g_{m-1}+A^*f'_{m-1}$$
$$-EcPr\Big[\sum_{n=0}^{m-1}f''_nf''_{m-1-n}-k_1\sum_{n=0}^{m-1}f''_{m-1-n}\Big(\sum_{i=0}^{n}f'_if''_{n-i}-\sum_{i=0}^{n}f_if'''_{n-i}\Big)\Big], \tag{3.10b}$$

and

$$\chi_m=\begin{cases}0, & \text{if } m\leq 1,\\ 1, & \text{if } m>1.\end{cases} \tag{3.11}$$

Eqs. (3.8a)-(3.8b) are linear nonhomogeneous differential equations that can be solved with symbolic computational software. Starting with the initial guesses in (3.2a)-(3.2b), $f_m(\eta)$ and $\theta_m(\eta)$ for $m\geq 1$ are obtained iteratively by solving (3.8a)-(3.9b). This procedure is terminated after a fixed number of iterations N to yield the approximate analytical solutions

$$f(\eta)\approx f_N(\eta)=\sum_{m=0}^{N}f_m(\eta), \tag{3.12a}$$

$$\theta(\eta)\approx\theta_N(\eta)=\sum_{m=0}^{N}\theta_m(\eta). \tag{3.12b}$$

4 Results and discussions

The convergence of the HAM solutions given in (3.12a)-(3.12b) depends on the convergence-control parameters $\hbar_f$ and $\hbar_\theta$, which are obtained using the Mathematica package BVPh 2.0 available at `http://numericaltank.sjtu.edu.cn/BVPh.htm`. Specifically, the discrete squared residuals defined by [7]

$$E^f_N(\hbar_f)=\frac{1}{M+1}\sum_{j=0}^{M}\Big\{\mathcal{N}_f\Big[\sum_{m=0}^{N}f_m(\eta_j)\Big]\Big\}^2, \tag{4.1a}$$

$$E^{\theta}_N(\hbar_f,\hbar_\theta)=\frac{1}{M+1}\sum_{j=0}^{M}\Big\{\mathcal{N}_\theta\Big[\sum_{m=0}^{N}f_m(\eta_j),\sum_{m=0}^{N}\theta_m(\eta_j)\Big]\Big\}^2, \tag{4.1b}$$

are minimized with respect to $\hbar_f$ and $\hbar_\theta$, where $\eta_j=0.1j$ and $M=100$ for the 20th-order approximations. The optimal values of the convergence-control parameters for all cases considered are obtained by first minimizing (4.1a) since it only depends on $\hbar_f$ and then substituting the optimal value of $\hbar_f$ into (4.1b) to find the optimal value of $\hbar_\theta$.

To demonstrate convergence of the HAM solutions, values of the physically relevant boundary derivatives and the discrete squared residuals are presented in Table 1 for different orders of approximation. Table 1 also includes values of the convergence-control parameters for default values of the system parameters.

Table 1: Convergence of the HAM solution for $k_1=0.2$, $Pr=3$, $Ec=0.25$, $A^*=-0.03$, $B^*=-0.03$, $\lambda=0$, $Nr=0$.

N	$-f''(0)$	E_N^f ($\hbar_f=-0.832$)	$-\theta'(0)$	E_N^θ ($\hbar_\theta=-0.415$)	$g(0)$	E_N^g ($\hbar_g=-0.406$)
5	1.1177256202229	1.410×10^{-8}	2.28051	1.262×10^{-3}	0.464719	1.062×10^{-3}
10	1.1180329886903	1.665×10^{-13}	2.31236	8.743×10^{-6}	0.471058	5.358×10^{-7}
15	1.1180339852165	2.360×10^{-18}	2.31451	4.138×10^{-7}	0.471011	5.750×10^{-8}
20	1.1180339887369	3.620×10^{-23}	2.31453	6.016×10^{-8}	0.470996	9.363×10^{-9}
25	1.1180339887498	5.794×10^{-28}	2.31456	1.154×10^{-8}	0.471002	1.843×10^{-9}
30	1.1180339887499	9.510×10^{-33}	2.31455	2.538×10^{-9}	0.471000	4.081×10^{-10}
35	1.1180339887499	1.587×10^{-37}	2.31455	6.116×10^{-10}	0.471000	9.801×10^{-11}
40	1.1180339887499	2.678×10^{-42}	2.31455	1.573×10^{-10}	0.471000	2.499×10^{-11}

Table 2: Comparison of values of wall temperature gradient (PST case) and wall temperature (PHF case). Default values of the parameters: $k_1=0.2$, $Pr=3$, $Ec=0.25$, $A^*=-0.03$, $B^*=-0.03$, $\lambda=0$, $Nr=0$.

Parameter	Value	$-\theta'(0)$ [1]	$-\theta'(0)$ (HAM)	$g(0)$ [1]	$g(0)$ (HAM)
	-0.03	2.34355	2.31455	0.459332	0.471001
A^*	0	2.30373	2.30373	0.475354	0.475354
	0.03	2.26392	2.29291	0.491373	0.479709
	-0.03	2.34355	2.31455	0.459332	0.471001
B^*	0	2.33742	2.30747	0.460336	0.472419
	0.03	2.33132	2.30037	0.461327	0.473851
	0.3	2.40941	2.29944	0.428081	0.472707
k_1	0.5	2.22889	2.25407	0.489054	0.478586
	0.7	2.14991	2.16101	0.498182	0.493337
	1	1.21628	1.25305	0.820812	0.807589
Pr	2	1.78304	1.85548	0.586958	0.567221
	3	2.34355	2.31455	0.459332	0.471001
	0	2.52479	2.49579	0.386396	0.398065
Ec	0.25	2.34355	2.31455	0.459332	0.471001
	0.5	2.07168	2.13331	0.530068	0.543937

Table 3: Default values of the parameters: $k_1=0.2$, $Pr=3$, $Ec=0.25$, $A^*=-0.03$, $B^*=-0.03$, $\lambda=0.5$, $Nr=1$.

Parameters	Values	$-f''(0)$ (PST)	$-f''(0)$ (PHF)	$-\theta'(0)$	$g(0)$
	1	0.87704	0.96236	1.64482	0.63594
Nr	2	0.84827	0.90661	1.31790	0.77734
	3	0.82689	0.85546	1.12465	0.89852
	-0.5	1.37399	1.29425	1.45070	0.694953
λ	0.5	0.87704	0.96236	1.64482	0.63594
	1	0.63733	0.81690	1.70696	0.61766

In Table 2 the values of $\theta'(0)$ and $g(0)$ computed with the HAM solutions are compared to the values in [1] that were obtained using Kummer's function in the absence of free convection. The results clearly do not agree requiring further analysis. To this end, it is useful to define the residual function

$$Res_{\hat\theta}(\eta)=(1+Nr)\hat\theta''+Pr\hat f\hat\theta'-2Pr\hat f'\hat\theta+EcPr(\hat f''^2+k_1\hat f''(\hat f'\hat f''-\hat f\hat f'''))+B^*\hat\theta+A^*\hat f', \quad (4.2)$$

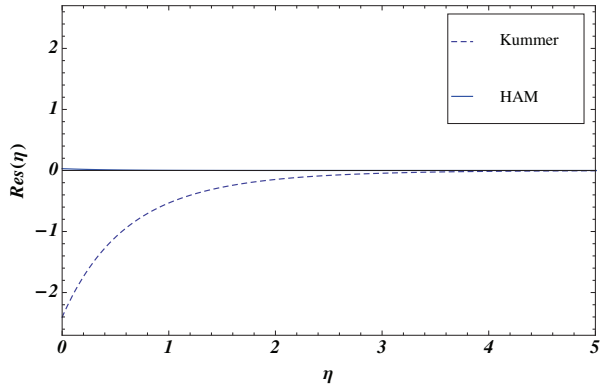

Figure 1: Residuals of the HAM solution and Kummer's function. Default values of the parameters: $k_1=0.2$, $Pr=3$, $Ec=0.25$, $A^*=-0.03$, $B^*=-0.03$, $\lambda=0$, $Nr=0$.

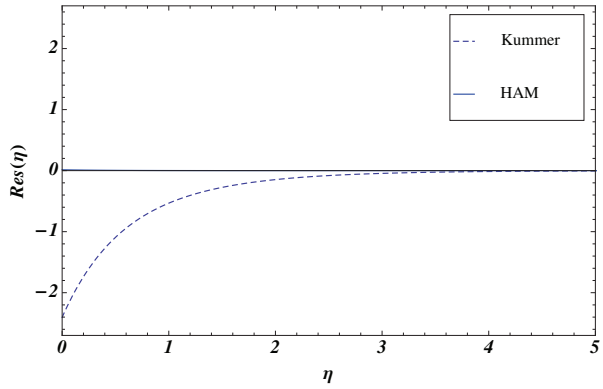

Figure 2: Residuals of the HAM solution and Kummer's function. Default values of the parameters: $k_1=0.2$, $Pr=3$, $Ec=0.25$, $A^*=-0.03$, $B^*=-0.03$, $\lambda=0$, $Nr=0$.

where $\hat{f}(\eta)$ and $\hat{\theta}(\eta)$ are approximate solutions to (2.10a) and (2.10b), respectively.

For both the PST and PHF cases, the HAM solution (3.12b) and the solution in terms of Kummer's function given in [1] are substituted into (4.2) and the results are plotted in Figs. 1-2. These figures provide convincing evidence that the solutions in terms of Kummer's function do not converge at the boundary, and therefore, the correct values of $\theta'(0)$ and $g(0)$ are given by the HAM solutions. In addition, Eqs. (2.10b) and (2.11b) are solved numerically as an initial value problem in which the unknown initial condition– $\theta'(0)$ for the PST case or $g(0)$ for the PHF case–is obtained from Table 2, and the solutions are plotted for both the PST and PHF cases in Figs. 3-4, respectively. It is clear that the numerical solutions obtained from initial conditions using Kummer's function do not have the proper limiting behavior as η approaches infinity, supporting the claim above. Finally, it is worth noting that solutions in terms of Kummer's function are only valid when there is no spatially dependent internal heat source/sink as evidenced in Table 2.

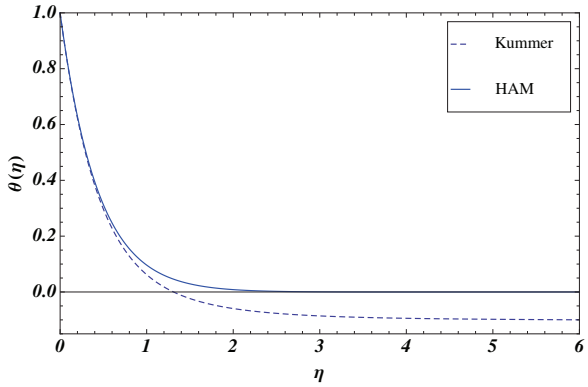

Figure 3: Comparison of HAM solution and Kummer's function for the PST case. Default values of the parameters: $k_1=0.2$, $Pr=3$, $Ec=0.25$, $A^*=-0.03$, $B^*=-0.03$, $\lambda=0$, $Nr=0$.

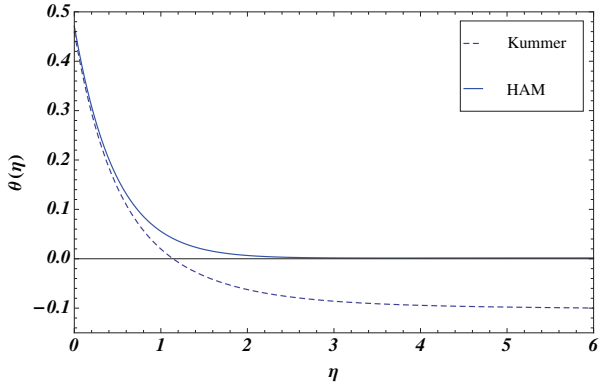

Figure 4: Comparison of HAM solution and Kummer's function for the PHF case. Default values of the parameters: $k_1=0.2$, $Pr=3$, $Ec=0.25$, $A^*=-0.03$, $B^*=-0.03$, $\lambda=0$, $Nr=0$.

In Figs. 5-8 the nondimensional velocity profiles are plotted for varying values of the free convection parameter and the thermal radiation parameter. It is evident that the boundary layer thickness increases as both of these parameters increase for either of the two types of thermal boundary conditions. In regard to free convection, these results mean that for assisting flow ($\lambda>0$) buoyancy forces act as a favorable pressure gradient whereas for opposing flow ($\lambda<0$) they act as an adverse pressure gradient.

Figs. 9-12 contain plots of the temperature profiles for varying values of the free convection parameter and the thermal radiation parameter. For either type of thermal boundary condition, the thermal boundary layer increases as the thermal radiation parameter increases, whereas an increase in the free convection parameter has the opposite effect. In Table 3 values of the physically relevant boundary derivatives are presented that support the aforementioned conclusions regarding the effects of the free convection parameter and the thermal radiation parameter on the momentum and thermal boundary layers. It is interesting to note that free convection has a greater effect on reducing

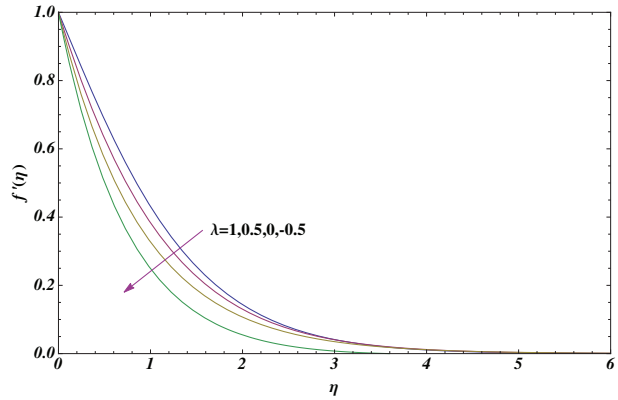

Figure 5: Velocity profiles for various values of λ for the PST case. Default values of the parameters: $k_1=0.2$, $Pr=3$, $Ec=0.25$, $A^*=-0.03$, $B^*=-0.03$, $\lambda=0.5$, $Nr=1$.

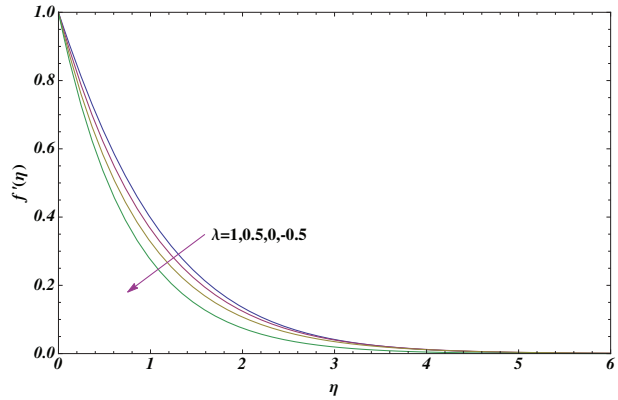

Figure 6: Velocity profiles for various values of λ for the PHF case. Default values of the parameters: $k_1=0.2$, $Pr=3$, $Ec=0.25$, $A^*=-0.03$, $B^*=-0.03$, $\lambda=0.5$, $Nr=1$.

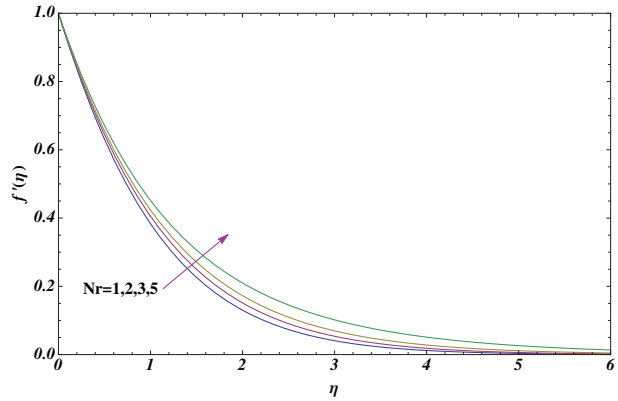

Figure 7: Velocity profiles for various values of Nr for the PST case. Default values of the parameters: $k_1=0.2$, $Pr=3$, $Ec=0.25$, $A^*=-0.03$, $B^*=-0.03$, $\lambda=0.5$, $Nr=1$.

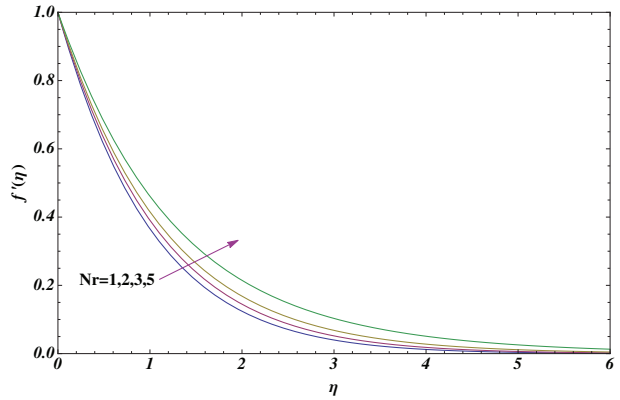

Figure 8: Velocity profiles for various values of Nr for the PHF case. Default values of the parameters: $k_1=0.2$, $Pr=3$, $Ec=0.25$, $A^*=-0.03$, $B^*=-0.03$, $\lambda=0.5$, $Nr=1$.

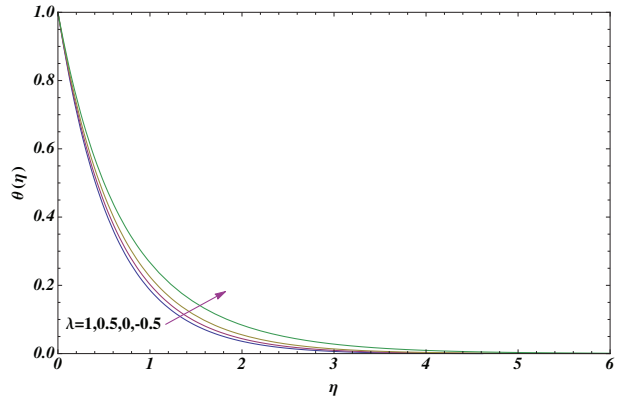

Figure 9: Temperature profiles for various values of λ for the PST case. Default values of the parameters: $k_1=0.2$, $Pr=3$, $Ec=0.25$, $A^*=-0.03$, $B^*=-0.03$, $\lambda=0.5$, $Nr=1$.

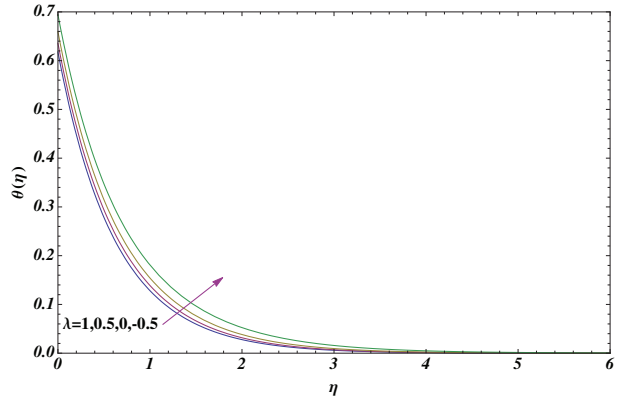

Figure 10: Temperature profiles for various values of λ for the PHF case. Default values of the parameters: $k_1=0.2$, $Pr=3$, $Ec=0.25$, $A^*=-0.03$, $B^*=-0.03$, $\lambda=0.5$, $Nr=1$.

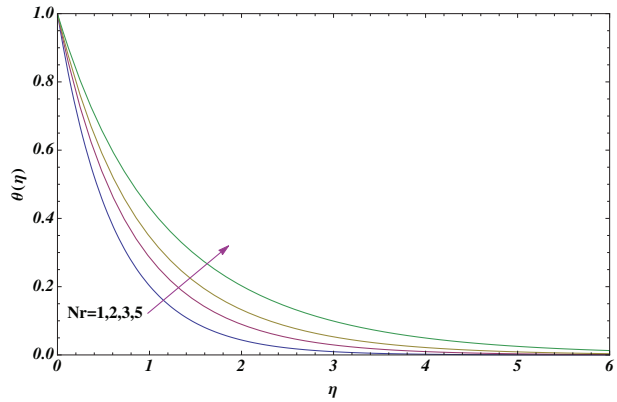

Figure 11: Temperature profiles for various values of Nr for the PST case. Default values of the parameters: $k_1=0.2$, $Pr=3$, $Ec=0.25$, $A^*=-0.03$, $B^*=-0.03$, $\lambda=0.5$, $Nr=1$.

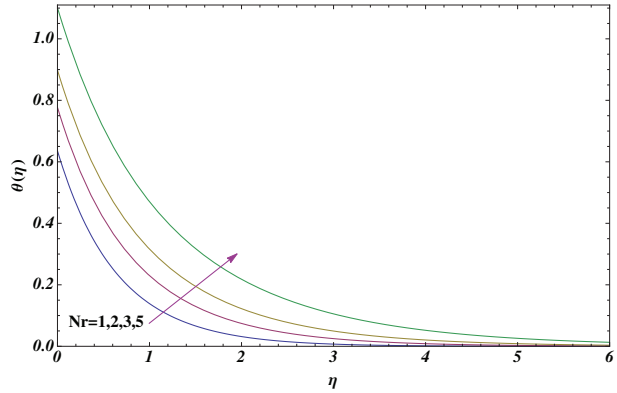

Figure 12: Temperature profiles for various values of Nr for the PHF case. Default values of the parameters: $k_1=0.2$, $Pr=3$, $Ec=0.25$, $A^*=-0.03$, $B^*=-0.03$, $\lambda=0.5$, $Nr=1$.

the magnitude of the skin friction coefficient for the PST case.

5 Conclusions

In this study, an analysis of mixed convection boundary layer flow of an incompressible and electrically conducting viscoelastic fluid over a linearly stretching surface in which the heat transfer includes the effects of viscous dissipation, elastic deformation, thermal radiation, and non-uniform heat source/sink for two general types of non-isothermal boundary conditions has been carried out. The nonlinear system of ordinary differential equations governing the fluid flow and heat transfer has been solved using the homotopy analysis method (HAM). Graphical and numerical demonstrations of the convergence of the HAM solutions have been provided, and the effects of various parameters on the skin friction coefficient and wall heat transfer have been tabulated. It has been clearly demonstrated that previously reported solutions of the thermal energy equation in the

presence of a non-uniform heat source/sink given in [1] do not converge at the boundary, and therefore, the boundary derivatives reported are not correct. Finally, velocity and temperature profiles have been plotted for various values of the parameters for both non-isothermal boundary conditions.

These results have significant implications on previously reported research in which Kummer's function has been used to represent solutions to the temperature field in the presence of a non-uniform heat source/sink. Because of its generality and versatility, HAM is a very effective analytical method for solving nonlinear problems in science and engineering that offers clear advantages over other analytical methods. As such it should be given serious consideration by researchers who seek analytical solutions to problems involving viscoelastic boundary flow and heat transfer.

References

[1] M. M. NANDEPPANAVAR, M. S. ABEL AND J. TAWADE, *Heat transfer in Walter's liquid B fluid over an impermeable stretching sheet with non-uniform heat source/sink and elastic deformation*, Commun. Nonlinear Sci. Numer. Simul., 15 (2010), pp. 1791–1802.
[2] H. BLASIUS, *Grenzschichten in Flussigkeiten mit kleiner Reibung*, Z. Math. Phys., 56 (1908), 137.
[3] S. J. LIAO, Proposed Homotopy Analysis Techniques for the Solution of Nonlinear Problems, Ph.D. dissertation, Shanghai Jiaotong University, Shanghai, 1992.
[4] S. J. LIAO, *A kind of approximate solution technique which does not depend upon small parameters II: an application in fluid mechanics*, Int. J. Nonlinear Mech., 32 (1997), pp. 815–822.
[5] S. J. LIAO, Beyond Perturbation: Introduction to the Homotopy Analysis Method, Chapman & Hall-CRC Press, Boca Raton, FL, 2003.
[6] S. J. LIAO, *Notes on the homotopy analysis method: some definitions and theorems*, Commun. Nonlinear Sci. Numer. Simul., 14 (2009), pp. 983–997.
[7] S. J. LIAO, *An optimal homotopy-analysis approach for strongly nonlinear differential equations*, Commun. Nonlinear Sci. Numer. Simul., 15 (2010), pp. 2003–2016.
[8] S. J. LIAO, Homotopy Analysis Method in Nonlinear Differential Equations, Springer & Higher Education Press, Heidelberg, 2012.
[9] A. MASTROBERARDINO, *Homotopy analysis method applied to electrohydrodynamic flow*, Commun. Nonlinear Sci. Numer. Simul., 16 (2011), pp. 2730–2736.
[10] A. MASTROBERARDINO, *Series solutions for annular axisymmetric stagnation flow on a moving cylinder*, Appl. Math. Mech., 34 (2013), pp. 1043–1054.
[11] B. C. SAKIADIS, *Boundary layer behavior on continuous solid surface: II-boundary layer on a continuous flat surface*, AIChE J, 7 (1961), pp. 221–225.
[12] L. J. CRANE, *Flow past a stretching plate*, Z. Angew. Math. Phys., 21 (1970), pp. 645–647.
[13] K. VAJRAVELU AND D. ROLLINS, *Heat transfer in a viscoelastic fluid over a stretching sheet*, J. Math. Anal. Appl., 158 (1991), pp. 241–255.
[14] M. S. SARMA AND B. N. RAO, *Heat transfer in a viscoelastic fluid over a stretching sheet*, J. Math. Anal. Appl., 222 (1998), pp. 268–275.
[15] K. M. C. PILLAI, K. S. SAI, N. S. SWAMY, H. R. NATARAJA, S. B. TIWARI AND B. N. RAO, *Heat transfer in a viscoelastic boundary layer flow through a porous medium*, Comput. Mech., 34 (2004), pp. 27–37.

[16] M. S. ABEL, P. G. SIDDHESHWAR AND M. M. NANDEPPANAVAR, *Heat transfer in a viscoelastic fluid flow over a stretching sheet with viscous dissipation and non-uniform heat source*, Int. J. Heat Mass Trans., 50 (2007), pp. 960–966.

[17] J. C. ARNOLD, A. A. ASIR, S. SOMASUNDARAM AND T. CHRISTOPHER, *Heat transfer in a viscoelastic boundary layer flow over a stretching sheet*, Int. J. Heat Mass Trans., 53 (2010), pp. 1112–1118.

[18] D. PAL AND H. MONDAL, *Influence of chemical reaction and thermal radiation on mixed convection heat and mass transfer over a stretching sheet in Darcian porous medium with Soret and Dufour effects*, Energy Convers Manage, 62 (2012), pp. 102–108.

[19] A. RAPTIS AND C. PERDIKIS, *Viscoelastic flow by the presence of radiation*, Z. Angew Math. Mech., 78 (1998), pp. 277–279.

[20] C. H. CHEN, *On the analytic solution of MHD flow and heat transfer for two types of viscoelastic fluid over a stretching sheet with energy dissipation, internal heat source and thermal radiation*, Int. J. Heat Mass Trans., 53 (2010), pp. 4264–4273.

[21] M. M. NANDEPPANAVAR, M. S. ABEL AND J. TAWADE, *Heat transfer in MHD viscoelastic boundary layer flow over a stretching sheet with thermal radiation and non-uniform heat source/sink*, Commun. Nonlinear Sci. Numer. Simul., 16 (2011), pp. 3578–3590.

[22] M. S. ABEL, K. V. PRASAD AND A. MAHABOOB, *Buoyancy force and thermal radiation effects in MHD boundary layer visco-elastic fluid flow over a continuously moving stretching surface*, Int. J. Therm. Sci., 44 (2005), pp. 465–476.

[23] A. MASTROBERARDINO AND U. S. MAHABALESWAR, *Mixed convection in viscoelastic flow due to a stretching surface in a porous medium*, J. Porous Media, 16 (2013), pp. 483–500.

[24] T. HAYAT, Z. ABBAS AND I. POP, *Mixed convection in the stagnation point flow adjacent to a vertical surface in a viscoelastic fluid*, Int. J. Heat Mass Trans., 51 (2008), pp. 3200–3206.

[25] T. HAYAT, M. MUSTAFA AND S. MESLOUB, *Mixed convection boundary layer flow over a stretching surface filled with a Maxwell fluid in presence of Soret and Dufour effects*, Z. Naturforsch, 65a (2010), pp. 401–410.

[26] Z. ABBAS, Y. WANG, T. HAYAT AND M. OBERLACK, *Mixed convection in the stagnation point flow of a Maxwell fluid towards a vertical stretching surface*, Nonlinear Anal. Real World Appl., 11 (2010), pp. 3218–3228.

[27] R. A. VAN GORDER AND K. VAJRAVELU, *Convective heat transfer in a conducting fluid over a permeable stretching surface with suction and internal heat generation/absorption*, Appl. Math. Comput., 217 (2011), pp. 5810–5821.

[28] T. HAYAT, M. HUSSAIN, S. NADEEM AND S. MESLOUB, *Falkner-Skan wedge flow of a power law fluid with mixed convection and porous medium*, Comput. Fluids, 49 (2011), pp. 22–28.

[29] T. HAYAT, S. A. SHEHZAD AND M. QASIM, *Mixed convection flow of a micropolar fluid with radiation and chemical reaction*, Int. J. Numer. Meth. Fluids, 67 (2011), pp. 1418–1436.

[30] D. W. BEARD AND K. WALTERS, *Elastico-viscous boundary-layer flows I: two-dimensional flow heat stagnation point*, Proc. Cambridge Philos. Soc., 60 (1964), pp. 667–674.

[31] H. I. ANDERSSON, *MHD flow of a visco-elastic fluid past a stretching surface*, Acta Mech., 95 (1992), pp. 227–230.

[32] M. Q. BREWSTER, Thermal Radiative Transfer and Properties, John Wiley & Sons, Canada, 1992.